Physico-mechanical performances of flax fiber biobased composites: Retting and process effects

Morgan Lecoublet, Mehdi Khennache, Nathalie Leblanc, Mohamed Ragoubi, Christophe Poilâne

Physico-mechanical performances of flax fiber biobased composites: Retting and process effects

Lecoublet Morgan[1], Khennache Mehdi[1], Leblanc Nathalie[1], Ragoubi Mohamed[1], Poilâne Christophe[2]

(1) : Unilasalle, Unité de Recherche Transformation et Agro-Ressources, VAM²IN (EA 7519 UniLaSalle – Université d'Artois), Mont-Saint-Aignan, France.
(2) : Normandie Univ, ENSICAEN, UNICAEN, CEA, CNRS, CIMAP, 14000 Caen, France

Corresponding author: mohamed.ragoubi@unilasalle.fr

Abstract

This research aimed to evaluate the effect of retting (3 levels were concerned) and processing parameters (mainly temperature) on physico-chemical properties of flax-epoxy materials. 9 biobased composites were produced with 3 different processing programs: Setup 1, 2, and 3. An advanced organoleptic study has been carried out on both technical flax fibers and manufactured composites to study in more detail the effects of the processing and retting on the visual aspect. Organoleptic analysis shows that flax, as well as biobased composites, lose saturation and luminance by increasing retting time. Increasing the processing temperature alters the material color. According to SEM analysis, we highlight that the least retted fibers are presented in bundles that are well bonded and coated with each other to form a technical fiber. Depending on retting, technical fibers appear cleaner and more individualized but their mechanical properties are affected. An interesting approach has been applied for the determination of the volumic content of our biobased composites, using both TGA and pycnometer methods. On average, V_f decreases from 63.1% for early retting (-) to 51.5% for late retting (+). This effect could naturally result from the observed individualization of the fibers. Moreover, the porosity rates V_p increase overall with fiber content. On average it varies from 5 to 11% in function of retting. Setup 3, with a processing temperature of 160°C, a processing time of 130 minutes and a processing pressure of 50 bars, is the most desirable because it allows the highest V_f for the lowest V_p. Regarding the mechanical behavior of biobased composites, we have observed a non-elastic behavior of our stress-strain curves, due to the intrinsic behavior of flax fibers. Stress *vs* strain curves reveal 3 different areas for elastic and plastic transitions. It also appears that setup 3 provides the best modulus of elasticity compared to the other setups. We notice also that E1 Young's modulus gradually increases with retting. By performing a normalization of E1 modulus according to the fiber volume, the effect of retting is even more pronounced. A 40% increase in modulus can be observed between retting (-) and (+). At the end, the long retting level of technical flax fibers, as well as the third setup gives the best compromise for our bio based composite performances.

Keywords

flax morphology, retting effect, flax biobased materials, mechanical performances (elasticity and rigidity), porosity rate

1. Introduction

In a context of emerging bioeconomy and sustainable development, biocomposites materials represent a niche in the industrial sector with strong dynamic growth. Materials science no longer counts the number of studies devoted to it. These materials have many advantages thanks to the intrinsic properties of natural fibers. The density of the latter being lower than that of glass or carbon (Le Gall et al., 2018; Amiri et al.,

2017), they are potential candidates for applications requiring structural lightenings such as the automobile (Akampumuza et al., 2017), aeronautics (Balakrishnan et al., 2016) and sport (Grande et al., 2018; Pailler et al., 2004).

Moreover, these natural reinforcements can be produced locally, depending on the climatic conditions (Bourmaud et al., 2018): flax (Haag et al., 2017; Khennache et al., 2019; Pallesen, 1996), hemp (Amaducci et al., 2015; Mazian et al., 2018; Marrot et al., 2013) for temperate climates, sisal, alfa (Hanana et al., 2015), date palm (Dhakal et al., 2018) and ramie (Rehman et al., 2019) for climates with higher temperatures, for example. Their intrinsic properties (chemical and physical) vary according to many parameters: crystallinity, cellulose content, number of walls in the cell, cellulose micro-fibrillar angles (Bourmaud et al., 2013, Bourmaud et al., 2018; Morvan et al., 2003; Cai et al., 2015 ...). These variables depend on their role in the plant. The best Young's moduli (characterizing their mechanical properties) are achieved with ramie fibers, with moduli between 60-128 GPa and fiber strength of 400-1480 MPa according to Giridharan, 2019 and Angelini et al., 2000, approaching glass fibers values. Among all these natural resources, flax is the most cultivated fiber plant in northern Europe (Martin et al., 2013). These fibers are not continuous like glass or carbon fibers. They have an average length between 2 and 5 cm (Morvan et al., 2003), tied together in a bundle structure made of 13 to 27 unitary fibers depending on the flax maturity and the position of the fibers in the plant (Morvan et al., 2003). They are bound together by cortical tissue made of pectin (Martin et al., 2013; Morvan et al., 2003). Young's moduli values for flax fibers are reported between 18 and 57 GPa according to Khennache et al., 2019. This great variability of results can easily be explained by protocols difference and materials used. Particular care must be taken by knowing precisely hygrometric conditions, length and cross-section of the technical fiber, variety of flax used, treatment applied, and its retting. According to several studies (Martin et al., 2013; Ruan et al., 2015), retting tends to improve Young's modulus, ultimate stress and reduce elongation at break for both field and water retting. This improvement has been associated with an increase in the percentage of cellulose, which is mainly responsible for plant rigidity. This improvement has been also observed in polypropylene-short fibers biobased composites, made by injection (Martin et al., 2013). For long fibers, most of the work is done with a thermosetting matrix-like epoxy, which is actually the matrix with the best mechanical properties. Fibers are either woven (twill, satin, plain ...) or unidirectional. Unidirectional applications logically give longitudinal modulus between matrix and fiber ones, according to the law of mixtures. For a 50% volumic fraction, Oksman, 2001 Kersani et al., 2015 and Coroller et al., 2013 reported Young's moduli from 27.2 to 39 GPa and maximum stresses from 296 to 408 MPa.

Despite extensive testing, a lot of development and optimization work will still be necessary for a larger industrialization scale. A major problem is the retting control, which highly depends on weather conditions. In the case of flax, the retting applied for biobased composite applications is the same as those used in the textile industry. However, there is no indication that this is the optimal retting process. We need optimal retted flax to improve the fiber-matrix interface without degradation of the fiber itself. Being of different nature compared to synthetic fiber, the organic fiber must have special processing and care to avoid structural defects in the associated composite. Porosity in the biobased composite is one of the defects that can result from poor processing. Porosities are defined as internal defects in a biocomposite structure and could have several origins (processing, fiber-matrix interface, residual moisture). To determine the porosity rates remains very complex according to the nature of involved porosity at different scale (macro, meso, micro …). For the porosity determination, several authors report qualitative (Ledru et al. 2009, Zhou et al. 1997, Lin et al. 2009) and quantitative X-Ray microtomography (Weber et al., 2010, Nikishkov et al., 2013), pycnometer (Consortium BioLAM, 2018) and mercury porosimeter (Ramakrishna

et al., 1988, Tran et al., 2015) technics. These two latter technics are the most suitable and efficient technics for porous biobased materials. To our knowledge, four main porosities are already existing: porosities coming from fiber, matrix, interface, and impregnation.

- i) The first type of porosity corresponds to the lumen's fiber. This porosity varies in size depending on the fiber's type. It can range from a few percent for flax fibers to 90% for kapok fibers, logically giving a variable rate of porosity in biocomposite using them.

- ii) Matrix porosities are due to two subtypes of porosities (Bodaghi et al., 2016; Grunenfelder and Nutt, 2010). Residual air and water present in the materials create gas inclusions, leading to porosities.

- iii) Porosities coming from the fiber-matrix interface are due to a poor interface between the fiber and the matrix. This may be due to a too low surface energy of fibers, compared to the matrix (Al-Khanbashi et al., 2005; Tran et al., 2015) or a presence of polluting compounds on fibers (Acera Fernández et al., 2016; Al-Khanbashi et al., 2005). They can also occur during the whole lifetime of composites, due to external mechanical stresses that favor fiber-matrix decohesion in areas with low impregnation.

- iv) Porosities coming from impregnation defects (structural porosities) are indirectly linked to fibers. These porosities appear if the matrix is not present enough to fill the free spaces of the biocomposite (Madsen et al., 2007). Structural porosity for a high fiber content biocomposite will be a major constituent. The curing cycle can induce structural defects. The organic nature of fibers will tend to increase this rate compared to inorganic fibers such as glass, as organic fibers contain a higher percentage of water (between 7 and 12%, Müssig et al., 2010).

For improving flax composite material knowledge and industrialization, this study focuses on Physico-chemical and mechanical studies of flax fiber reinforcements and their epoxy composites manufactured by thermocompression. Retting and processing parameters have been studied to examine their impacts on flax fibers and bio-based composite materials in terms of morphological aspect, mechanical performance, and porosity rate. To determine the different rates (fibre, matrix and water) in our biobased composites, an interesting approach has been applied. This method relies on the use of TGA analysis to determine the weight contents of the flax fibers, the matrix, the water and a pycnometer to determine the porosity rate.

2. Materials and Methods

2.1. Raw materials

Flax cultivation – Bolshoi variety – has been established in Romilly-la-Puthenay, Normandie, based on a well-established agricultural process. Flax was seeded on April 10th, 2017, and harvested on July 13th, 2017 as indicated in **Table 1**. The latter date was chosen according to the sum of the cumulative degrees received by the plants, 1014°C, which gives the maturity level of fibers. Winding dates were based on visual estimation of the retting level (**Figure 1**), according to climatic conditions. **Figure 2** shows the different levels of retting on the flax tapes. Consequently, the first winding date W1 was set for August 7th, 2017. Because windrows were not too thick, it was possible to have homogeneous retting without any turn-over. The two other winding dates W2 and W3 were set on August 28th (1 turn-over) and September

22th (2 turn-overs). The flax was then scutched to separate flax fibers from the stems. No hackling steps were carried out, nor any thermal, chemical, or physical preparations.

(Insertion of Table 1 here)

(Insertion of Figure 1 here)

(Insertion of Figure 2 here)

The matrix used is an epoxy XB 3515/Aradur 5021. XB 3515 is a high-temperature epoxy resin and Aradur 5021 is a polyamine curing agent. It was used as delivered and according to the manufacturer's recommendation for the curing process.

2.2. Preparation of biobased composites

Once the flax has been scutched, it receives a pre-impregnation step by Vitech Composite society. The average fiber mass fraction is given as 50 % ± 3. The matter is then kept in our laboratory in a -18°C room.

Three different protocols based on thermocompression molding were tested, without any post-curing. Elaboration programs are explained in detail in **Figure**s **3a** to **3c**. The first protocol (**Figure 3a**) is the actual program used by our industrial partner and has been studied to be optimized in terms of temperature, time, and pressure (**Figure 3b**).

(Insertion of Figure 3a at 3c here)

For the elaboration step, prepregs stored in the refrigerator, are cut into 30 cm squares (**Figure 4a**), stacked in a unidirectional pattern of 3-plys, and placed between two 3mm thick metal plates. Teflon films are used to facilitate the demolding step (**Figure 4b**). **Table 2** summarizes the given names to composites, processing variables, and first measurement of thickness and mass per unit area. Retting (-) corresponds to under-retted flax, retting (0) corresponds to nominally retted flax for textile applications and retting (+) corresponds to over-retted flax.

(Insertion of Table 2 here)

(Insertion of Figure 4a and 4b here)

2.3. Methods used.

All the following graphics have been made using Matlab software and Python Programming Language with the Matplotlib, Numpy, and Pandas modules.

2.3.1. Spectrophotometry analysis

Spectrophotometry is traditionally used to determine the absolute color of materials. A Konica Minolta CM 2300d spectrophotometer analysis was carried out to quantify the color of raw materials (flax) and biobased composites materials. The coordinates systems are expressed in the CIE 1976 Colorspace (**Figure 5**):

- i) L* coordinate expresses the lightness of the color, ranging from 0 (black) to 100 (white).
- ii) a* coordinate expresses the green-red component. Negative values result in green colors and positive ones for red colors.
- iii) Finally, the b* coordinate expresses the blue-yellow component. Negative values result in blue colors and positive ones for yellow colors.

(Insertion of Figure 5 here)

Moreover, for the components a* and b*, the larger the value, the more saturated the color will be. Whiteness Index W* is the distance between a specified color and a perfect white, expressed in the CIELab Colorspace (Pérez et al., 2016). It was calculated using the following equation (**Eq.1**)

$$W^* = \sqrt{(L^* - 100)^2 + a^{*2} + b^{*2}} \ (\mathbf{Eq.1})$$

Where W* is the Whiteness Index, L* is the component L*, a* is the component a*, and b* the component b*. Each result will be an average of 10 measurements and expressed in the CIE Lab 1976 color space.

2.3.2. Scanning Electronic Microscopy (SEM)

Scanning Electronic Microscopy (SEM) analysis was carried out to observe flax fiber and biobased composite morphology. The tests were conducted under 15kV with magnification ranging from x37 to x200. All the composite samples were polished with a #1000 sanding paper. No coating was applied to either material. Three specimens were analyzed for each material.

2.3.3. DSC analysis

Differential scanning calorimetry (DSC) was used to observe phase transitions in materials by heat exchange. A DSC Polyma DSC 214 was used to determine the monomer conversion rate of the different biobased composites. The program consists of two heating ramps ranging from 25°C to 250°C at 10°C. min^{-1}, with an argon flow of 20ml.min^{-1}. The second heating is used to check the total conversion of monomers. The resin used for the manufacture of prepregs was compared to these values. The matrix conversion rate was calculated using the following equation (**Eq.2**)

$$\alpha = \left(\frac{\frac{dH_c}{W_m}}{dH_r} \right) * 100 \ (\mathbf{Eq.2})$$

Where α is the monomer conversion rate, dH_c is the exothermic peak of the composite, W_m is the weight matrix content of the composite, and dH_r the exothermic peak of the resin, derived from Konuray et al., 2017. Each result is an average of 3 measurements made with 10-15 mg of material.

2.3.3. TGA analysis

TGA is usually used to observe the thermal stability of the material. As part of this study, it was used to determine the fiber content of biobased composites. The method is based on the studies of Yee and Stephens, 1996, and Mohsin et al., 2019. The method consists of a set of isotherm (i) 1st isotherm of 165°C for 30 minutes (to remove the water contained by the fibers) and (ii) 2nd isotherm of 325°C for 60 min. This duration (60 min) is the more suitable among 4 different tested durations (20, 40, 60 and 90 min), as shown in **Figure 6**.

(Insertion of Figure 6 here)

For TGA analysis, an argon flow of 20ml.min^{-1} was used. Three specimens were tested for each condition. The theoretical weight fiber content of the composite (W_f) was determined using the following equations (**Eq.3**) and (**Eq.4**)

$$W_f = \frac{\Delta_{composite} - \Delta_{matrix}}{\Delta_{fiber} - \Delta_{matrix}} \quad \textbf{(Eq. 3)}$$

$$W_m = 100 - W_f - W_w \quad \textbf{(Eq.4)}$$

Where $\Delta_{composite}$ is the composite loss, Δ_{matrix} is the matrix loss, Δ_{fiber} is the fiber loss, W_f is the weight fiber content of the composite, W_m is the weight matrix content of the composite, and W_w the weight water content of the composite assumed to be the water loss of the composite, observed with TGA data. $\Delta_{composite}$ and Δ_{matrix} was determined with the neat

Then, to determine the volumic content of the different components, equation (**Eq. 5**), derived from Ahmed and Vijayarangan., 2008 and Sanjay and Yogesha., 2018 was used:

$$V_f = \frac{\frac{W_f}{\rho_f}}{\frac{W_f}{\rho_f} + \frac{W_m}{\rho_m} + \frac{W_w}{\rho_w}} \quad \textbf{(Eq.5)}$$

Where V_f is the volumic fiber content of the composite, W_f is the weight fiber content of the composite, W_m is the weight matrix content of the composite, W_w is the weight water content of the composite, ρ_f is the density of the fiber, ρ_m is the density of the matrix and ρ_w the density of the water.

2.3.4. Pycnometer analysis

The pycnometer is usually used to determine the fiber levels by comparing the density of raw materials and composite but assuming a material with 0% void, which is not the case in our study. Then the porosity rate could be calculated, indirectly. Pycnometer analysis was carried out to calculate the density of the biobased composites. Three specimens were tested for each condition. Once the theoretical and

experimental density has been calculated, the porosity rate was calculated using the equation (**Eq. 6**) proposed by Yee and Stephens., 1996.

$$Porosity\ rate = \left(\frac{Theorical\ density - Experimental\ density}{Theorical\ density}\right) \textbf{(Eq.6)}$$

2.3.5. Tensile test for flax fibers

Mechanical tests were carried out by using an MTS Criterion 43 tensile machine. Tested lengths range from 14 to 100 mm, with 2 mm increments (thirty-three samples by retting mode). The displacement rate was set at 1 mm.min^{-1}. This part was conducted in the frame of Khennache Ph.D study and the first results were published in Khennache et al., 2019. It is important to note that a new method was used to determine the average cross-section of each technical fiber by weighing and accurate knowledge of sample density.

2.3.6. Tensile test for biobased composite materials

Tensile tests were carried out on a Shimadzu traction machine with a 50 kN capacity load and self-tightening jaws. The displacement rate was fixed at 2 mm.min^{-1} and carried out at 23°C and 65% HR. Dog bone specimens, prepared according to ISO 527, were cut by a laser beam with a cutting speed of 35 mm.s^{-1} (**Figure 7a**). Flax-epoxy plates were glued at the area pinched by the jaws to avoid early breaks (**Figure 7b**). For each material, five samples were tested.

(Insertion of Figure 7a and 7b here)

3. Results

3.1. Spectrophotometry and morphological analysis of flax fibers

Figure 8 shows the variation of the L*a*b* components for flax modalities with different levels of retting (under-retted, nominally retted, and over-retted). As we can see, there is a significant decrease of the L* components, (from 57.3 to 54.1), a* (from 4.0 to 2.7), and b* (from 21.8 to 13.0) depending on retting. This result is visually reflected in a transition from yellow to grey respectively for the less retted (-) and the more retted (+) flax. Similar observations and trends have also been reported by Pallesen, 1996 and Martin et al., 2013 for flax fibers, by Mazian et al., 2018 for hemp fibers, and Bleuze et al., 2018 for hemp stems. Quantitatively, the results are like those observed by Martin et al., 2013 and Bleuze et al., 2018. Compared to these studies, the slight color variations may be due to several reasons: the type of fiber, the used variety, and the level of applied retting. It should be noted that Chabbert et al., 2020 observed an increase of the L* component and an increase, rapidly followed by a decrease on the a* and b* components for dew-retted flax.

(Insertion of Figure 8 here)

Moreover, **Figure 8** illustrates that color transition is not a single phase. Indeed, the color transition from retting (-) to retting (0) seems different from the color transition from retting (0) to retting (+). This first transition only reduces saturation without significantly altering clarity (P-value > 0.05). This could be associated with possible degradation of the soluble components present in flax fibers. In fact, Van Soest results – not presented here – show that soluble components decrease according to the retting levels. The obtained values are 10.4% (± 0.5), 6.1% (± 0.3) and 4.5% (± 1.1) which corresponds respectively to the

levels (-), (0) and (+). Statistical analysis shows that the difference between these results is significant (ANOVA results showed that the P-value is equal to 1.58 $x10^{-4}$). The transition from retting (0) to retting (+) is marked by a decrease of clarity and a slight loss of b* component. This transition could be attributed to the colonization of the fiber by a microbial biofilm (Mazian et al., 2018), thus promoting the individualization of elementary fibers.

Figure 9 shows the SEM pictures obtained for fiber modalities at different levels of retting. It is important to note that the least retted fibers (-) are presented in bundles that are well bonded and coated with each other to form a technical fiber. Cohesion is potentially ensured by soluble compounds (pectins, fats, and wax) according to Morvan et al., 2003 and Meijer et al., 1995. Depending on retting, this coating tends to disappear and leave the fiber's surface more visible according to Martin et al., 2013. These results are also confirmed for enzymatic retting of flax fibers (Réquilé et al., 2018; Ruan et al., 2020), hemp fibers (Li et al., 2009; Liu et al., 2015), and date palm fibers (Chaari et al., 2020). Elementary fibers are perfectly visible for retting (+) and therefore better individualized. It should be noted that the fibers with the longest retting (+) do not appear to be visually degraded.

(Insertion of Figure 9 here)

3.2. Tensile analysis of flax fibers

For tensile analysis, different measurements were carried out on flax fibers and allowed us to deduce two observations:

- i) When the fiber length tends towards 0 mm, the technical fiber is close to a huge continuous elementary fiber. Its mechanical behaviors tend to that of elementary fiber,

- ii) When the fiber length reaches 100 mm and over, its mechanical behavior is that of long technical fiber, i.e. a sum of elementary fibers linked by pectins.

Young's modulus, tensile strength, and failure strain of technical fiber (when the fiber length reaches 0 and 100 mm) are given in **Table 3**. It should be noted that in the case of fiber length assimilated to 0 mm, retting tends to have a double effect: a positive one on fiber stiffness and a negative one on ultimate stress. Retting leads to elementary fiber's dissociation from each other, leading to cleaner fiber surfaces and more spaced fibers as shown by SEM results (**Figure 9**) and reported elsewhere by Khennache et al., 2019; Martin et al., 2013, Nair et al., 2014 and Bourmaud et al., 2019.
In this case, the rigidity of technical fibers being the mean rigidity of all the elementary fibers (length 0 mm). At the same time, the fiber section decreases by cleaning effect during the scutching. Therefore, the ratio L/d increases and allows a positive effect on the rigidity. Conversely, the negative effect of retting on the ultimate strength could be explained by the lack of interface and the lack of stress – transfer provided by the middle lamella.

(Insertion of Table 3 here)

When the fiber length is assimilated to 100mm, all the mechanical properties decrease when the retting increases. **Table 3** shows a 15% decrease in Young's modulus and nearly 50% of the ultimate stress was observed. Internal forces are no longer transmitted by the coat made of pectins, reducing drastically the strength and the rigidity of technical fibers. All these elements and the well-known not only elastic

behavior of elementary flax fiber (Poilâne et al., 2014; Keryvin et al., 2015; Richard et al., 2018), result in not linear and not elastic behavior of flax technical fiber.

3.3. Spectrophotometry analysis of biobased composites

Figure 10 shows L*a*b* measurements for biobased composites obtained by setup 1. It can be pointed out that the components (L*, a*, b*) tend to decrease for the biobased materials. It indicates that the resulting color for the materials rather converges towards a dark color (a color that turns brown as shown in **Figures 4** and **5**. It seems that the same trends already observed for flax fibers are also observed for epoxy/flax materials. Compared to the flax fibers, it seems that for biobased composites, L* and b* components tend to decrease while the a* component increases, which is in correlation with the color transition towards a soft brown color. As the retting effect remains clearly visible on flax reinforcement, we highlight that the epoxy resin, which has a transparent aspect once crosslinked, seems to not affect the color transition of biobased materials, essentially at 140°C.

(Insertion of Figure 10 here)

More concretely, **Figure 11** shows in 3D the L*a*b* components of flax and flax-epoxy biobased composite obtained with the different setups (1, 2, 3). It shows that for setups 1 and 2 (temperature at 140°C), the color of the biobased composite displays the same trend such as for flax. This would indicate a weak effect of processing parameters (time and pressure) applied during implementation for these setups. This could be attributed to the softening and decomposition of soluble products (pectins and waxes) contained in flax fibers. However, a strong color transition is visible for biobased materials made with setup 3 which could be directly associated with step-up temperature (160°C). To check the effect of setup temperature, two additional bio-based composite plates were prepared with less retting (-) flax and with a processing temperature of 80 and 190°C.

(Insertion of Figure 11 here)

Figure 12 shows a* and Whiteness W* components as a function of the processing temperature. It should be noted that whatever the temperature, the W* component increases continuously. However, the a* component increases steadily until it reaches a threshold from 160°C. Visually, the processing temperature (temperature varies from 80 to 190°C) induces a color variation (a color translation from yellow-orange-red and finally a brown color) of the biobased composite plates. Perhaps this temperature-dependent color variation is due to a chemical reaction induced by the processing step and the biochemical composition and nature of fibers and matrix. Further studies and analysis are still in progress to understand and explain these phenomena.

(Insertion of Figure 12 here)

3.4. Volumic determination of biobased composites

Table 4 provides experimental weight and volumic fractions of the different components (fibers, matrix, porosity, and water) constituting the biobased composites. The volumic fiber fraction (V_f) ranges from 48.2 to 66.7% and the volumic porosity rate (V_p) ranges from 4.9 to 11.3%. These results show better efficiency for setup 3 because of higher V_f and lower V_p compared to Setups 1 and 2. Furthermore, the V_f

and the V_p decrease with the retting level which leads to more compact materials. This could be attributed to a possible improvement of the fiber surfaces due to the retting action, as already observed with SEM.

(Insertion of Table 4 here)

Figure 13 shows the V_p as a function of the V_f rate. It shows that despite significant variability, V_p increases overall with V_f. These observations confirm that setup 3 seems to be optimal regarding porosity (higher V_f for the lowest V_p). Our results have porosity rates identical to those observed by Yang, 2017, Berges et al., 2016 and Hallonet et al., 2019 with a higher V_f, ranging from 48.2 to 66.8%. The results were confirmed by image analysis (not presented here), giving approximately the same order.

(Insertion of Figure 13 here)

3.5. Curing efficiency

Figure 14 shows the percentage of non-converted monomers, calculated according to **Eq.2** described in the "materials and methods" section. We would like to notice that the DSC study was found to be difficult to obtain reproducible results associated mainly with low homogeneity of biobased composites. Standard deviations vary between 6 and 52%.

(Insertion of Figure 14 here)

However, it appears that the percentage of unconverted monomers varies mainly with the setup used. Setup 1 seems to convert monomers better than setups 2 and 3. It also seems that the conversion rate is only marginally affected by the retting of the fibers (**Figure 14b**). Indeed, although the best conversion rates are obtained for retting (-) for setup 1 and retting (+) for setups 2 and 3, the results are not statistically relevant (P-value between 0.47 and 0.53). As could be observed, the percentage of unconverted monomers varies greatly depending on the setups used. The lowest percentages 2.9 (±1.6) of unconverted monomers are obtained with the biobased composites in setup 1 while the highest percentages 9.1 (±0.9) of unconverted monomers are obtained with the biobased composites in setup 3. This difference could be explained by the processing time, the shorter the curing time, the higher the unconverted monomers. Similar results have been mentioned in the literature (Granado et al., 2018; Teyssandier et al., 2010) and confirm that less processing time leads to a less conversion rate. From these findings, it will be necessary to apply post-curing treatment to allow better resin crosslinking and optimizing the corresponding properties of biobased materials.

3.6. Mechanical analysis of biobased composites

Figure 15a shows typical stress-strain curves for our biobased composite materials. The observed behavior is typical for flax-based composites loading and has been fully described in the literature (Scida et al., 2013; Poilâne et al., 2014; Richard et al., 2018; Cadu et al., 2019; Bourmaud et al., 2016). The observed failures at the end of the tests were typically longitudinal breaks. Its initiation has been attributed to interfacial fractures between fibers and matrix by Rask et al., 2012. The values deduced from the stress *vs* strain curves are reported in **Table 5**.

(Insertion of Table 5 here)

(Insertion of Figure 15a and 15b here)

Based on the raw values, elastic property analysis reveals 3 areas (illustrated in **Figure 15b**). Area 1 (0-0.1%) is elastic, Young's modulus, E1, is the initial slope in that area. Area 2 (0.1-0.3%) is a transition area and could be attributed to a rapid rearrangement of the amorphous phase of S2 associated with the arrangement of crystalline cellulose microfibrils resulting in a decrease of rigidity from area 1 to area 3, as already reported by Hughes et al., 2007 and Bensadoun et al., 2017. Area 3 (over 0.3%) presents not only elastic behavior, final secant modulus, E2, and ultimate stress – also called strength – are computed in that area. The non-elastic behavior of polymer reinforced by plant fibers is not fully understood, it was globally explained by microstructural damage potentially accompanied by inelastic or viscoelastic behavior (Hughes et al., 2007) due to the intrinsic non-linearity of the elementary fibers (Bensadoun et al., 2017).

Figure 16 shows E1, E2 moduli, and tensile strength associated with the different biobased composites manufactured. We observe that E1 gradually increases with retting. It also appears that setup 3 provides the best modulus of elasticity compared to the two other setups. The lowest Young's modulus is 14.3 (± 0.6) GPa for setup 2 (-) and the best Young's modulus is 19.5 (± 0.9) GPa for setup 3 (+). Contrastingly, E2 modulus varies between 11.1 (± 0.4) and 14.2 (± 0.6) GPa, which is 25% lower than Young's modulus. Setup 3 still seems to allow the best rigidity values, but the effect of setup and retting is not very high for E2 modulus. The effects of process and retting on tensile strength are not so simple. The tensile strength increases with retting for setup 3, but normal retting is better for setups 1 and 2. The lowest tensile strength, 251 (± 16) MPa, is obtained for setup 3 (-) and the best, 381 (± 32) MPa, for setup 3 (+).

(Insertion of Figure 16 here)

It appears from the previous results that the long retting mode associated with the third setup gives the best compromise for our composite performances. For this setup, the morphological analysis of technical fibers shows optimal elementary fiber individualization. Spectrophotometry analysis of fibers could confirm this quality of fibers dissociation, which is an interesting lead for retting quantification in the field. Indeed, growers look for a scientific method able to quantify the retting in the field before harvesting. However, the porosity rate, which is one of the keys of composite performances, decreases with retting and with setup (according to the setup numbering), giving the lower value also for setup 3 (+). The fiber rate increases with the setup but decreases with the retting; it is due to the facility for the matrix to diffuse between elementary fibers which present the better individualization for long retting. Consequently, the higher specific surface of the fiber-matrix interface is obtained for setup 3 (+). It is another key for composite performances, particularly efficient when the length of fibers is compatible with load transfer, which is the case with elementary fibers as with technical fibers. Note that the third setup is shorter than setup 2 which is shorter than setup 1. It results that the percentage of non-converted monomers increases with setup (see §3.2.4); consequently, one specific post-curing of composites – which has not been applied here – would increase the observed difference of performances, which would result in better performances for setup 3.

The raw values of strength are typical for such flax composites with a high fraction of fibers. But the raw values of modulus are particularly weak. For unidirectional flax/epoxy composite, Cherif et al., 2013 measured 26.3 GPa for $V_f = 44\%$ and Richard et al., 2018 identified 30.7 GPa for $V_f = 47\%$. We recall that no specific preparation of flax except scutching was done before impregnation and that no post-curing of plates has been done.

The aim of this work is not to obtain the best performances but to compare three degrees of retting and three processes of elaboration of flax composite plates. SEM analysis performed on 2 (-) composite specimens is presented **in Figure 17**. The orientation of the fibers is normal to the observation. We clearly identify epoxy matrix in grey, flax fibers in light grey – with a lumen in the form of thin lines in the fibers themselves, the fibers being flattened, as reported in other works (Le Gall et al., 2018; Madsen et al., 2007; Mahboob et al., 2017) – and various types of porosity in dark grey, including dry areas. We also note some artifacts, foreign matters, or saturated areas that appear in white. Matrix porosities have not been seen, either by their absence or by their small size. The largest dry area, highlighted in **Figure 17b** represents 1/3 of specimen thickness. The numerous interfacial porosities highlighted in **Figure 17d** result in very weak flax-epoxy interfaces. We assume that the weak flax-epoxy interfaces due to the use of raw flax and the high level of percentage of unconverted monomers in the matrix explain the low moduli of the elaborated composite plates. Indeed, studying results for quasi-unidirectional composites with the same order of porosity in literature (Cherif et al., 2016, Scida et al., 2012), we conclude that the global rate of porosity itself can not explain the low modulus of the elaborated composites.

(Insertion of Figure 17a at 17d here)

Furthermore, to highlight the efficiency of the retting process, it is necessary to normalize the raw mechanical properties by porosity and fiber contents using the law of mixture. We have chosen to apply the inverse method described by Cherif et al., 2016, which gives the reinforcement efficiency knowing resin and composite properties including porosity rate. For infinite unidirectional composite, the effective Young's modulus of reinforcement and its effective ultimate strength is given by (**Eq.7**) and (**Eq.8**), respectively:

$$E_{ff} = \frac{E_C*(1-V_p)^{-2} - E_m*V_m}{V_f} \quad \textbf{(Eq.7)}$$

$$\sigma_{ff} = \frac{\sigma_C*(1-V_p)^{-2}}{V_f + V_m*\frac{E_m}{E_C}} \quad \textbf{(Eq.8)}$$

Where E_{ff} is the fiber effective Young's modulus, E_c is the composite Young's modulus, E_m is the matrix Young's modulus, V_f is the volumic fiber content of the composite, V_m is the volumic matrix content of the composite, V_p is the volumic porosity content of the composite, σ_{ff} is the fiber effective ultimate strength and σ_c is the effective ultimate strength of the composite.

The resulting effective properties are given in **Table 5**. **Figure 18** shows the evolution of the effective modulus and strength of the reinforcement as a function of retting and process. It is clear that retting has a positive impact on the mechanical performance of flax fibers once used as a reinforcement in composite, the longer the retting process the higher the mechanical efficiency of reinforcement. This observation has also been made by Martin et al., 2013. Nevertheless, the values of modulus presented in section 3.2 for the fibers prove that the efficiency of the reinforcement is not optimal for our composites, as we noted in the previous paragraph. Indeed, the effective modulus of the reinforcement computed by an inverse method is much lower than that of elementary flax fiber as well as that of long technical fiber. Oppositely, the effective ultimate stress of the reinforcement is in the same order of magnitude as that of elementary flax fiber, and higher than that of long technical fiber.

(Insertion of Figure 18a and 18b here)

The difficulty on relying on composite properties to reinforcement properties by the law of mixture is well known for plant fiber composites (Shah et al., 2016) and it is why a research effort is necessary to describe plant fiber behavior by phenomenological approach (Poilâne et al., 2014; Richard et al., 2018). Concerning the inverse approach from the law of mixture, note that the strength and the modulus of the composite focus on two opposite phases of reinforcement deformation: the modulus is measured at the beginning of the strain, when not all the fibers are activated, a lot of them is not already stretched (depending to the efficiency of the flax-epoxy interfaces); the strength is measured at the end of the strain when all the elementary fibers are stretched but not at the same step of their behavior (not only elastic) and lot of them have been already broken or dissociated. Nevertheless, an increase up to 37% in effective modulus and 75% in effective strength can be observed by the simple used approach between retting (-) and (+) for setup 3. The elementary fiber individualization is responsible for this property's improvement with retting. The true benefit of setup 3 is more difficult to analyze here. It could be due to the elimination of the initial 20 bar/25°C-plateau – which can locally stress the resin too much at a temperature where it is not very fluid – or to 160°C-maximal temperature – where the flax fiber is submitted to huge modifications which can be positive to increase the efficiency of flax/epoxy interface. Further physicochemical analysis will be required to explore these hypotheses.

4. Conclusion

In this study, physico-mechanical performances of 3-layer flax-epoxy biobased composites manufactured by thermocompression were studied, and more particularly the retting and processing effect. From a morphological point of view, retting tends to individualize the technical fibers bundles into single ones. This individualization phenomenon could be attributed to a possible degradation of middle lamella allowing a cleaner and smoother surface of fibers and affecting their final mechanical properties (15% decrease of Young's modulus, 50% decrease of the ultimate stress). Increasing retting time leads to a lose saturation and luminance, both for flax and biobased materials. However, increasing the processing temperature alters the material color. More particularly, the composite weight fiber (W_f) tends to decrease as a function of retting level for all setups. This effect could naturally result from the observed individualization of the fibers and would therefore lead to a reduction in their compactness, which makes easier the penetration of resin (lead to better resin impregnation). Moreover, the porosity rate, which is one of the keys of composite performances, decreases with the retting and with the used setups (according to the setup numbering), giving the lower value also for setup 3 (+). Consequently, the higher specific surface of the fiber-matrix interface is obtained for setup 3 (+). It is another key for composite performances, particularly efficient when the length of fibers is compatible with load transfer, which is the case with elementary fibers as with technical fibers.

Regarding the mechanical behavior and based on the raw values, elastic properties of flax biobased composite reveal three different areas for elastic and plastic transitions, as already reported in the literature. The raw values of tensile strength are typical for such flax composites with a high fraction of fibers, but the raw values of elastic modulus are particularly weak because of the low composite plate cross-linking obtained with manufacturer recommendation for the curing process. However, the resulting effective properties show that retting has a positive impact on the mechanical performance of flax composite, the longer the retting process the higher the mechanical efficiency of reinforcement. The elementary fiber individualization is responsible for this property's improvement with retting. Nevertheless, the values of fiber modulus prove that the efficiency of reinforcement is not optimal for our

composites. Indeed, the effective modulus of the reinforcement computed by the inverse method is much lower than that of elementary flax fiber as well as that of long technical fiber. Conversely, the effective ultimate stress of the reinforcement is in the same order of magnitude as that of elementary flax fiber, and higher than that of long technical fiber. The long retting mode associated with the third setup gives the best compromise for our composite performances. Furthermore, physico-chemical analyses are necessary to confirm the nature of chemical reactions happening during the curing and manufacture of flax composites structure.

Acknowledgments

The authors thank all academic and industrial partners of the OLCO project (FEDER-17P04941), particularly the Normandy region and FEDER for their financial support.

References

Acera Fernández, J., Le Moigne, N., Caro-Bretelle, A.S., El Hage, R., Le Duc, A., Lozachmeur, M., Bono, P., Bergeret, A., 2016. Role of flax cell wall components on the microstructure and transverse mechanical behavior of flax fabrics reinforced epoxy biocomposites. Ind. Crops Prod. 85, 93–108. https://doi.org/10.1016/j.indcrop.2016.02.047

Ahmed, K.S., Vijayarangan, S., 2008. Tensile, flexural, and interlaminar shear properties of woven jute and jute-glass fabric reinforced polyester composites. J Mater Process Technol. 207, 330–335. https://doi.org/10.1016/j.jmatprotec.2008.06.038

Akampumuza, O., Wambua, P.M., Ahmed, A., Li, W., Qin, X.-H., 2017. Review of the applications of biocomposites in the automotive industry: Review of the Applications of Biocomposites in the Automotive Industry. Polym Compos. 38, 2553–2569. https://doi.org/10.1002/pc.23847

Al-Khanbashi, A., Al-Kaabi, K., Hammami, A., 2005. Date palm fibers as polymeric matrix reinforcement: Fiber characterization. Polym Compos. 26, 486–497. https://doi.org/10.1002/pc.20118

Amaducci, S., Scordia, D., Liu, F.H., Zhang, Q., Guo, H., Testa, G., Cosentino, S.L., 2015. Key cultivation techniques for hemp in Europe and China. Ind. Crops Prod. 68, 2–16. https://doi.org/10.1016/j.indcrop.2014.06.041

Amiri, A., Triplett, Z., Moreira, A., Brezinka, N., Alcock, M., Ulven, C.A., 2017. Standard density measurement method development for flax fiber. Ind. Crops Prod. 96, 196–202. https://doi.org/10.1016/j.indcrop.2016.11.060

Angelini, L.G., Lazzeri, A., Levita, G., Fontanelli, D., Bozzi, C., 2000. Ramie (Boehmeria ni6ea (L.) Gaud.) and Spanish Broom (Spartium junceum L.) fibres for composite materials: agronomical aspects, morphology, and mechanical properties. Ind. Crops Prod. 11, 145–161. https://doi.org/10.1016/S0926-6690(99)00059-X

Balakrishnan, P., John, M.J., Pothen, L., Sreekala, M.S., Thomas, S., 2016. Natural fiber and polymer matrix composites and their applications in aerospace engineering, in Advanced Composite Materials for Aerospace Engineering. Elsevier, pp. 365–383. https://doi.org/10.1016/B978-0-08-100037-3.00012-2

Bensadoun, F., Verpoest, I., Baets, J., Müssig, J., Graupner, N., Davies, P., Gomina, M., Kervoelen, A., Baley, C., 2017. Impregnated fiber bundle test for natural fibers used in composites. J Reinf Plast Compos. 36, 942–957. https://doi.org/10.1177/0731684417695461

Berges, M., Léger, R., Placet, V., Person, V., Corn, S., Gabrion, X., Rousseau, J., Ramasso, E., Ienny, P., Fontaine, S., 2016. Influence of moisture uptake on the static, cyclic, and dynamic behavior of unidirectional flax fiber-reinforced epoxy laminates. Composites, Part A. 88, 165–177. https://doi.org/10.1016/j.compositesa.2016.05.029

Bleuze, L., Lashermes, G., Alavoine, G., Recous, S., Chabbert, B., 2018. Tracking the dynamics of hemp dew retting under controlled environmental conditions. Ind. Crops Prod. 123, 55–63. https://doi.org/10.1016/j.indcrop.2018.06.054

Bodaghi, M., Cristóvão, C., Gomes, R., Correia, N.C., 2016. Experimental characterization of voids in high fiber volume fraction composites processed by high injection pressure RTM. Composites, Part A. 82, 88–99. https://doi.org/10.1016/j.compositesa.2015.11.042

Bourmaud, A., Beaugrand, J., Shah, D.U., Placet, V., Baley, C., 2018. Towards the design of high-performance plant fiber composites. Prog Mater Sci. 97, 347–408. https://doi.org/10.1016/j.pmatsci.2018.05.005

Bourmaud, A., Le Duigou, A., Gourier, C., Baley, C., 2016. Influence of processing temperature on mechanical performance of unidirectional polyamide 11–flax fiber composites. Ind. Crops Prod. 84, 151–165. https://doi.org/10.1016/j.indcrop.2016.02.007

Bourmaud, A., Morvan, C., Bouali, A., Placet, V., Perré, P., Baley, C., 2013. Relationships between micro-fibrillar angle, mechanical properties, and biochemical composition of flax fibers. Ind. Crops Prod. 44, 343–351. https://doi.org/10.1016/j.indcrop.2012.11.031

Bourmaud, A., Siniscalco, D., Foucat, L., Goudenhooft, C., Falourd, X., Pontoire, B., Arnould, O., Beaugrand, J., Baley, C., 2019. Evolution of flax cell wall ultrastructure and mechanical properties during the retting step. Carbohydr Polym. 206, 48–56. https://doi.org/10.1016/j.carbpol.2018.10.065

Cadu, T., Van Schoors, L., Sicot, O., Moscardelli, S., Divet, L., Fontaine, S., 2019. Cyclic hygrothermal ageing of flax fibers' bundles and unidirectional flax/epoxy composite. Are bio-based reinforced composites so sensitive? Ind. Crops Prod. 141, 111730. https://doi.org/10.1016/j.indcrop.2019.111730

Cai, M., Takagi, H., Nakagaito, A.N., Katoh, M., Ueki, T., Waterhouse, G.I.N., Li, Y., 2015. Influence of alkali treatment on internal microstructure and tensile properties of abaca fibers. Ind. Crops Prod. 65, 27–35. https://doi.org/10.1016/j.indcrop.2014.11.048

Chaari, R., Khlif, M., Mallek, H., Bradai, C., Lacoste, C., Belguith, H., Tounsi, H., Dony, P., 2020. Enzymatic treatments effect on the poly (butylene succinate)/date palm fibers properties for bio-composite applications. Ind. Crops Prod. 148, 112270. https://doi.org/10.1016/j.indcrop.2020.112270

692 Chabbert, B., Padovani, J., Djemiel, C., Ossemond, J., Lemaître, A., Yoshinaga, A., Hawkins, S., Grec, S.,
693 Beaugrand, J., Kurek, B., 2020. Multimodal assessment of flax dew retting and its functional impact on
694 fibers and natural fiber composites. Ind. Crops Prod. 148, 112255.
695 https://doi.org/10.1016/j.indcrop.2020.112255
696
697 Cherif, Z.E., Poilâne, C., Falher, T., Vivet, A., Ouail, N., Doudou, B.B., Chen, J., 2013. Influence of
698 textile treatment on mechanical and sorption properties of flax/epoxy composites. Polym Compos. 34,
699 1761–1773. https://doi.org/10.1002/pc.22580
700
701 Cherif, Z.E., Poilâne, C., Vivet, A., Ben Doudou, B., Chen, J., 2016. About optimal architecture of plant
702 fibre textile composite for mechanical and sorption properties. Compos Struct. 140, 240–251.
703 https://doi.org/10.1016/j.compstruct.2015.12.030
704
705 Consortium BioLAM, 2018. Composites biosourcés & porosités : essais interlaboratoires. Presented at the
706 Biobased Laminates Research Consortium, Paris.
707
708 Coroller, G., Lefeuvre, A., Le Duigou, A., Bourmaud, A., Ausias, G., Gaudry, T., Baley, C., 2013. Effect
709 of flax fibres individualisation on tensile failure of flax/epoxy unidirectional composite. Composites, Part
710 A. 51, 62–70. https://doi.org/10.1016/j.compositesa.2013.03.018
711
712 Dhakal, H., Bourmaud, A., Berzin, F., Almansour, F., Zhang, Z., Shah, D.U., Beaugrand, J., 2018.
713 Mechanical properties of leaf sheath date palm fiber waste biomass reinforced polycaprolactone (PCL)
714 biocomposites. Ind. Crops Prod. 126, 394–402. https://doi.org/10.1016/j.indcrop.2018.10.044
715
716 Giridharan, R., 2019. Preparation and property evaluation of Glass/Ramie fibers reinforced epoxy hybrid
717 composites. Composites, Part B. 167, 342–345. https://doi.org/10.1016/j.compositesb.2018.12.049
718
719 Granado, L., Kempa, S., Gregoriades, L.J., Brüning, F., Genix, A.-C., Fréty, N., Anglaret, E., 2018.
720 Kinetic regimes in the curing process of epoxy-phenol composites. Thermochim Acta 667, 185–192.
721 https://doi.org/10.1016/j.tca.2018.07.019
722
723 Grande, D.H., Greist, S., Jessie, T., Daniel, J., 2018. 3.18 Composites in Sports Applications, in:
724 Comprehensive Composite Materials II. Elsevier, pp. 469–526. https://doi.org/10.1016/B978-0-12-
725 803581-8.10341-8
726
727 Grunenfelder, L.K., Nutt, S.R., 2010. Void formation in composite prepregs – Effect of dissolved
728 moisture. Compos Sci Technol. 70, 2304–2309. https://doi.org/10.1016/j.compscitech.2010.09.009
729
730 Haag, K., Padovani, J., Fita, S., Trouvé, J.-P., Pineau, C., Hawkins, S., De Jong, H., Deyholos, M.K.,
731 Chabbert, B., Müssig, J., Beaugrand, J., 2017. Influence of flax fiber variety and year-to-year variability
732 on composite properties. Ind. Crops Prod. 98, 1–9. https://doi.org/10.1016/j.indcrop.2016.12.028
733
734 Hallonet, A., Ferrier, E., Michel, L., Benmokrane, B., 2019. Durability and tensile characterization of wet
735 lay-up flax/epoxy composites used for external strengthening of RC structures. Constr Build Mater. 205,
736 679–698. https://doi.org/10.1016/j.conbuildmat.2019.02.040
737

738 Hanana, S., Elloumi, A., Placet, V., Tounsi, H., Belghith, H., Bradai, C., 2015. An efficient enzymatic-
739 based process for the extraction of high-mechanical properties alfa fibers. Ind. Crops Prod. 70, 190–200.
740 https://doi.org/10.1016/j.indcrop.2015.03.018
741
742 Hughes, M., Carpenter, J., Hill, C., 2007. Deformation and fracture behavior of flax fiber-reinforced
743 thermosetting polymer matrix composites. J Mater Sci. 42, 2499–2511. https://doi.org/10.1007/s10853-
744 006-1027-2
745
746 Kersani, M., Lomov, S.V., Van Vuure, A.W., Bouabdallah, A., Verpoest, I., 2015. Damage in flax/epoxy
747 quasi-unidirectional woven laminates under quasi-static tension. J Compos Mater. 49, 403–413.
748 https://doi.org/10.1177/0021998313519282
749
750 Keryvin, V., Lan, M., Bourmaud, A., Parenteau, T., Charleux, L., Baley, C., 2015. Analysis of flax fibers
751 viscoelastic behavior at micro and nanoscales. Composites, Part A. 68, 219–225.
752 https://doi.org/10.1016/j.compositesa.2014.10.006
753
754 Khennache, M., Mahieu, A., Ragoubi, M., Taibi, S., Poilâne, C., Leblanc, N., 2019. Physicochemical and
755 Mechanical Performances of Technical Flax Fibers and Biobased Composite Material: Effects of Flax
756 Transformation Process. J Renewable Mater. 7, 821–838. https://doi.org/10.32604/jrm.2019.06772
757
758 Konuray, A.O., Fernández-Francos, X., Ramis, X., 2017. Latent curing of epoxy-thiol thermosets.
759 Polymer. 116, 191–203. https://doi.org/10.1016/j.polymer.2017.03.064
760
761 Le Gall, M., Davies, P., Martin, N., Baley, C., 2018. Recommended flax fiber density values for
762 composite property predictions. Ind. Crops Prod. 114, 52–58.
763 https://doi.org/10.1016/j.indcrop.2018.01.065
764
765 Ledru, Y., Piquet, R., Michel, L., Schmidt, F., Bernhart, G., 2009. Quantification 2-D et 3-D de la porosité
766 par analyse d'images dans les matériaux composites stratifiés aéronautiques 12. hal-01851827
767
768 Li, Y., Pickering, K.L., Farrell, R.L., 2009. Analysis of green hemp fiber-reinforced composites using bag
769 retting and white-rot fungal treatments. Ind. Crops Prod. 29, 420–426.
770 https://doi.org/10.1016/j.indcrop.2008.08.005
771
772 Lin, L., Luo, M., Guo, G., Li, X., 2009. Ultrasonic determination of carbon fiber composite porosity using
773 acoustic impedance. Acta Materiae Compositae Sinica. 26, 105-110.
774
775 Liu, M., Fernando, D., Daniel, G., Madsen, B., Meyer, A.S., Ale, M.T., Thygesen, A., 2015. Effect of
776 harvest time and field retting duration on the chemical composition, morphology, and mechanical
777 properties of hemp fibers. Ind. Crops Prod. 69, 29–39. https://doi.org/10.1016/j.indcrop.2015.02.010
778
779 Madsen, B., Thygesen, A., Lilholt, H., 2007. Plant fiber composites – porosity and volumetric interaction.
780 Compos Sci Technol. 67, 1584–1600. https://doi.org/10.1016/j.compscitech.2006.07.009
781
782 Mahboob, Z., El Sawi, I., Zdero, R., Fawaz, Z., Bougherara, H., 2017. Tensile and compressive damaged
783 response in Flax fiber reinforced epoxy composites. Composites, Part A. 92, 118–133.
784 https://doi.org/10.1016/j.compositesa.2016.11.007
785

786 Marrot, L., Lefeuvre, A., Pontoire, B., Bourmaud, A., Baley, C., 2013. Analysis of the hemp fiber
787 mechanical properties and their scattering (Fedora 17). Ind. Crops Prod. 51, 317–327.
788 https://doi.org/10.1016/j.indcrop.2013.09.026
789
790 Martin, N., Mouret, N., Davies, P., Baley, C., 2013. Influence of the degree of retting of flax fibers on the
791 tensile properties of single fibers and short fiber/polypropylene composites. Ind. Crops Prod. 49, 755–767.
792 https://doi.org/10.1016/j.indcrop.2013.06.012
793
794 Mazian, B., Bergeret, A., Benezet, J.-C., Malhautier, L., 2018. Influence of field retting duration on the
795 biochemical, microstructural, thermal, and mechanical properties of hemp fibers harvested at the
796 beginning of flowering. Ind. Crops Prod. 116, 170–181. https://doi.org/10.1016/j.indcrop.2018.02.062
797
798 Meijer, W.J.M., Vertregt, N., Rutgers, B., van de Waart, M., 1995. The pectin content as a measure of the
799 retting and rettability of flax. Ind. Crops Prod. 4, 273–284. https://doi.org/10.1016/0926-6690(95)00041-0
800
801 Mohsin, M.A.A., Iannucci, L., Greenhalgh, E.S., 2019. Fibre-volume-fraction measurement of carbon
802 fiber reinforced thermoplastic composites using thermogravimetric analysis. Heliyon 5, e01132.
803 https://doi.org/10.1016/j.heliyon.2019.e01132
804
805 Morvan, C., Andème-Onzighi, C., Girault, R., Himmelsbach, D.S., Driouich, A., Akin, D.E., 2003.
806 Building flax fibres: more than one brick in the walls. Plant Physiol Biochem. 41, 935–944.
807 https://doi.org/10.1016/j.plaphy.2003.07.001
808
809 Müssig, J., Fischer, H., Graupner, N., Drieling, A., 2010. Testing Methods for Measuring Physical and
810 Mechanical Fibre Properties (Plant and Animal Fibres), in Müssig, J. (Ed.), Industrial Applications of
811 Natural Fibres. John Wiley & Sons, Ltd, Chichester, UK, pp. 267–309.
812 https://doi.org/10.1002/9780470660324.ch13
813
814 Nair, G.R., Kurian, J., Yaylayan, V., Rho, D., Lyew, D., Raghavan, G.S.V., 2014. Microwave-assisted
815 retting and optimization of the process through chemical composition analysis of the matrix. Ind. Crops
816 Prod 52, 85–94. https://doi.org/10.1016/j.indcrop.2013.10.007
817
818 Nikishkov, Y., Airoldi, L., Makeev, A., 2013. Measurement of voids in composites by X-ray Computed
819 Tomography. Composites Science and Technology 89, 89–97.
820 https://doi.org/10.1016/j.compscitech.2013.09.019
821
822 Oksman, K., 2001. High-Quality Flax Fibre Composites Manufactured by the Resin Transfer Moulding
823 Process. J Reinf Plast Compos. 20, 621–627. https://doi.org/10.1177/073168401772678634
824
825 Pailler, D., Sautreuil, P., Piera, J.-B., Genty, M., Goujon, H., 2004. Évolution des prothèses des sprinters
826 amputés de membre inférieur. Annales de Réadaptation et de Médecine Physique 47, 374–381.
827 https://doi.org/10.1016/j.annrmp.2004.05.007 (In French)
828
829 Pallesen, B.E., 1996. The quality of combine-harvested fiber flax for industrials purposes depends on the
830 degree of retting. Ind. Crops Prod. 5, 65–78. https://doi.org/10.1016/0926-6690(95)00049-6
831

Pérez, M. del M., Ghinea, R., Rivas, M.J., Yebra, A., Ionescu, A.M., Paravina, R.D., Herrera, L.J., 2016. Development of a customized whiteness index for dentistry based on CIELAB color space. Dent Mater. 32, 461–467. https://doi.org/10.1016/j.dental.2015.12.008

Poilâne, C., Cherif, Z.E., Richard, F., Vivet, A., Ben Doudou, B., Chen, J., 2014. Polymer reinforced by flax fibers as a viscoelastoplastic material. Compos Struct. 112, 100–112. https://doi.org/10.1016/j.compstruct.2014.01.043

Ramakrishna T. Bhatt, 1988. Properties of Silicon Carbide Fiber- Reinforced Silicon Nitride Matrix Composites, presented at the International Conference on Whisker- and Fiber-Toughened Ceramics sponsored by the American Society for Metals Oak Ridge, Tennessee

Rask, M., Madsen, B., Sørensen, B.F., Fife, J.L., Martyniuk, K., Lauridsen, E.M., 2012. In situ observations of microscale damage evolution in unidirectional natural fiber composites. Composites, Part A. 43, 1639–1649. https://doi.org/10.1016/j.compositesa.2012.02.007

Rehman, M., Gang, D., Liu, Q., Chen, Y., Wang, B., Peng, D., Liu, L., 2019. Ramie, a multipurpose crop: potential applications, constraints, and improvement strategies. Ind. Crops Prod. 137, 300–307. https://doi.org/10.1016/j.indcrop.2019.05.029

Réquilé, S., Le Duigou, A., Bourmaud, A., Baley, C., 2018. Peeling experiments for hemp retting characterization targeting biocomposites. Ind. Crops Prod. 123, 573–580. https://doi.org/10.1016/j.indcrop.2018.07.012

Richard, F., Poilâne, C., Yang, H., Gehring, F., Renner, E., 2018. A viscoelastoplastic stiffening model for plant fiber unidirectional reinforced composite behavior under monotonic and cyclic tensile loading. Compos Sci Tech. 167, 396–403. https://doi.org/10.1016/j.compscitech.2018.08.020

Ruan, P., Raghavan, V., Du, J., Gariepy, Y., Lyew, D., Yang, H., 2020. Effect of radiofrequency pretreatment on enzymatic retting of flax stems and resulting fibers properties. Ind. Crops Prod. 146, 112204. https://doi.org/10.1016/j.indcrop.2020.112204

Ruan, P., Raghavan, V., Gariepy, Y., Du, J., 2015. Characterization of Flax Water Retting of Different Durations in Laboratory Condition and Evaluation of Its Fiber Properties. BioResources 10, 3553–3563. https://doi.org/10.15376/biores.10.2.3553-3563

Sanjay, M., Yogesha, B., 2018. Studies on hybridization effect of jute/kenaf/E-glass woven fabric epoxy composites for potential applications: Effect of laminate stacking sequences. Journal of Industrial Textiles 47, 1830–1848. https://doi.org/10.1177/1528083717710713

Scida, D., Assarar, M., Poilâne, C., Ayad, R., 2013. Influence of hygrothermal ageing on the damage mechanisms of flax-fiber reinforced epoxy composite. Composites, Part B. 48, 51–58. https://doi.org/10.1016/j.compositesb.2012.12.010

Shah, D.U., Nag, R.K., Clifford, M.J., 2016. Why do we observe significant differences between measured and 'back-calculated properties of natural fibers? Cellulose 23, 1481–1490. https://doi.org/10.1007/s10570-016-0926-x

Teyssandier, F., Ivanković, M., Love, B.J., 2010. Modeling the effect of the curing conversion on the dynamic viscosity of epoxy resins cured by an anhydride curing agent: Dynamic Viscosity of Epoxy Resins. J Appl Polym Sci. 115, 1671–1674. https://doi.org/10.1002/app.31148

Tran, L.Q.N., Yuan, X.W., Bhattacharyya, D., Fuentes, C., Van Vuure, A.W., Verpoest, I., 2015. Fiber-matrix interfacial adhesion in natural fiber composites. Int J Mod Phys B. 29, 1540018. https://doi.org/10.1142/S0217979215400184

Weber, E., Fernandez, M., Wapner, P., Hoffman, W., 2010. Comparison of X-ray micro-tomography measurements of densities and porosity principally to values measured by mercury porosimetry for carbon-carbon composites. Carbon 48, 2151–2158. https://doi.org/10.1016/j.carbon.2009.11.047

Yang, H., Study of a unidirectional flax reinforcement for biobased composite. Mechanics of the solides [physics.class-ph]. Normandie Université, 2017. English. NNT: 2017NORMC226. tel-01663572

Yee, R.Y., Stephens, T.S., 1996. A TGA technique for determining graphite fiber content in epoxy composites. Thermochim Acta 272, 191–199. https://doi.org/10.1016/0040-6031(95)02606-1

Zhou, X., Mo, J., You, H., 1997. Ultrasonic attenuation testing method for NDE of void content based on theoretical model and experiment calibration. Acta Materiae Compositae Sinica 14, 107-114.

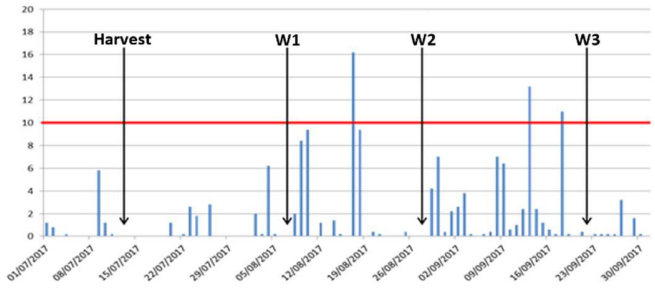

Figure 1: Winding dates based on visual estimation of the retting level and according to climatic conditions

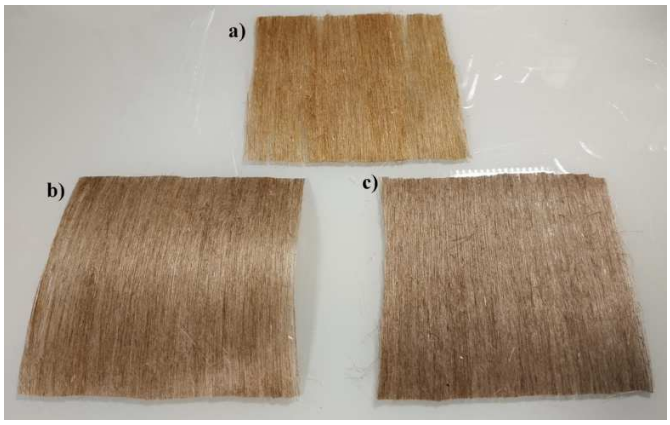

Figure 2: a) Under-retted flax, b) Retted flax, c) Over-retted flax

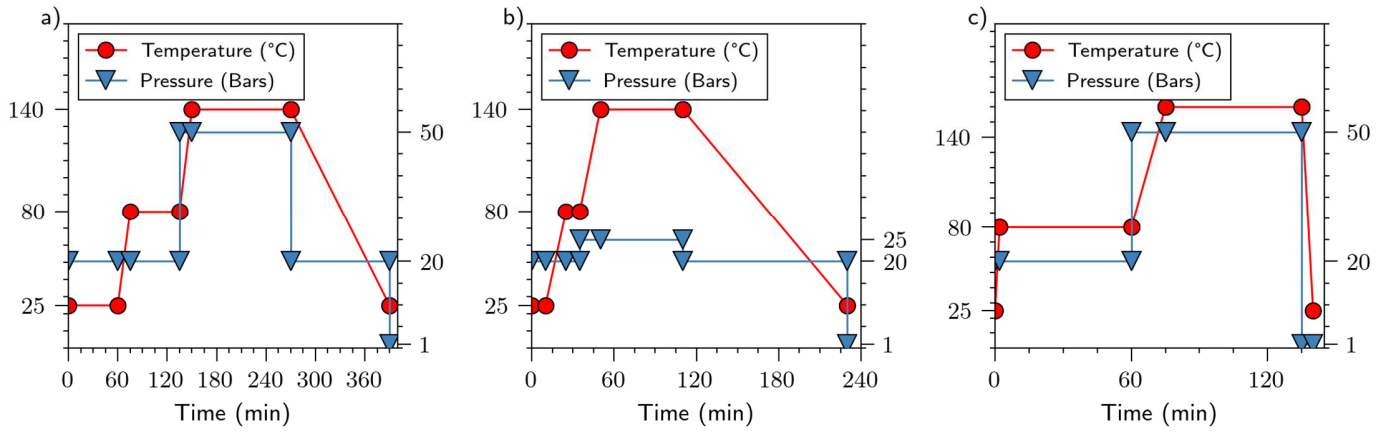

Figure 3: Biobased composites processing program a) Program 1, b) Program 2, c) Program 3

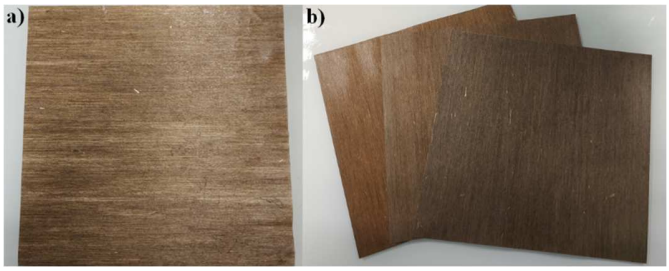

Figure 4: Biobased composites a) Prepreg of flax fibers, b) Flax-epoxy biobased composites

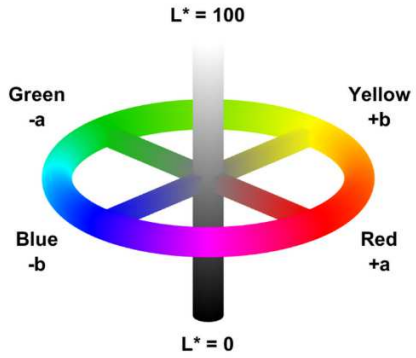

Figure 5: CIELab color space (Made with Matlab software)

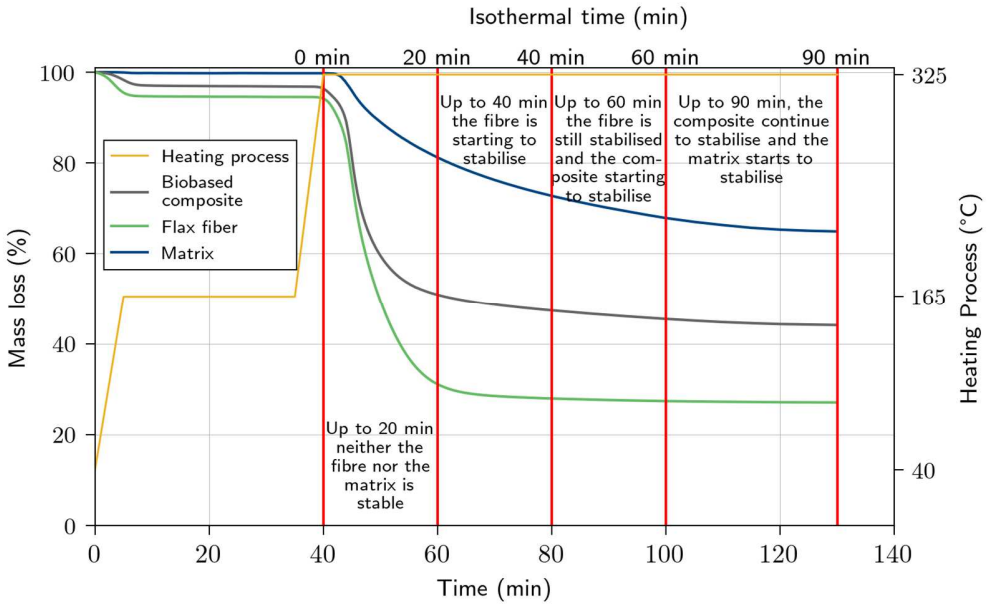

Figure 6 : TGA isothermal curves for flax fiber, matrix and Bio based composites

Figure 7: Flax-epoxy tensile test specimens a) general shape b) zoom on the grip section.

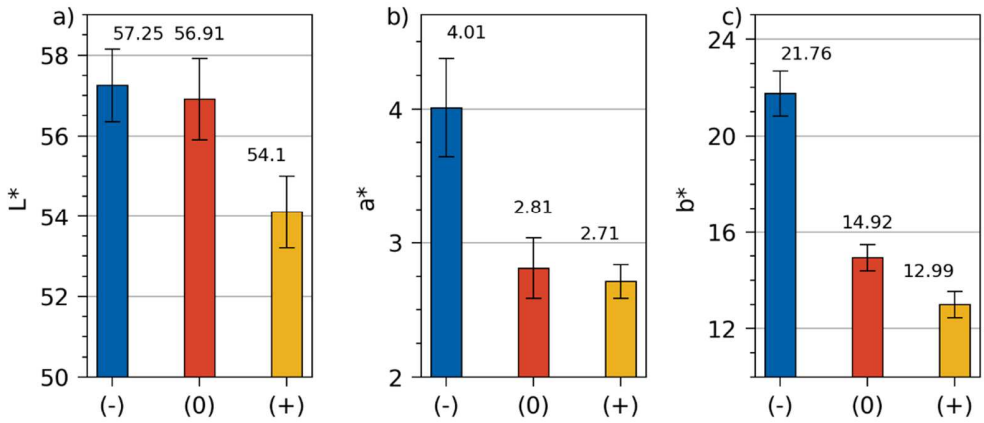

Figure 8: L*a*b* component for flax modalities at different retting

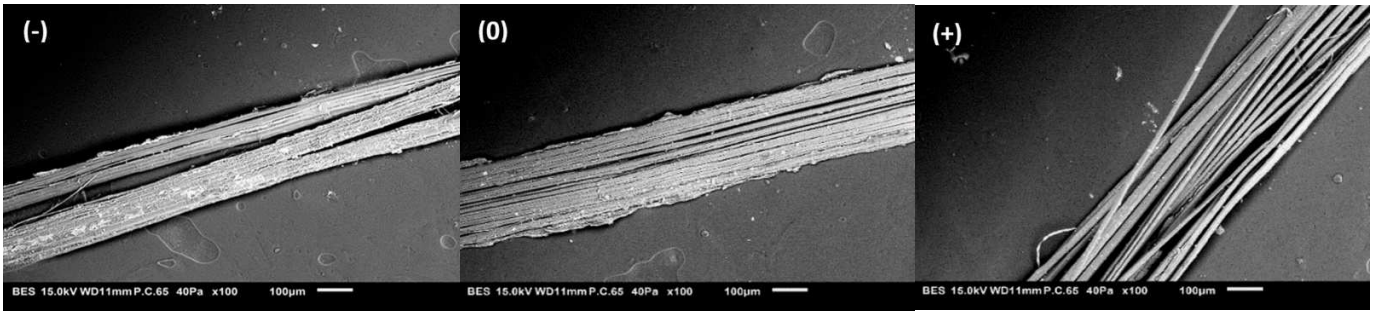

Figure 9: SEM pictures of flax technical fibres a) retting (-), b) retting (0), c) retting (+), (magnification x100)

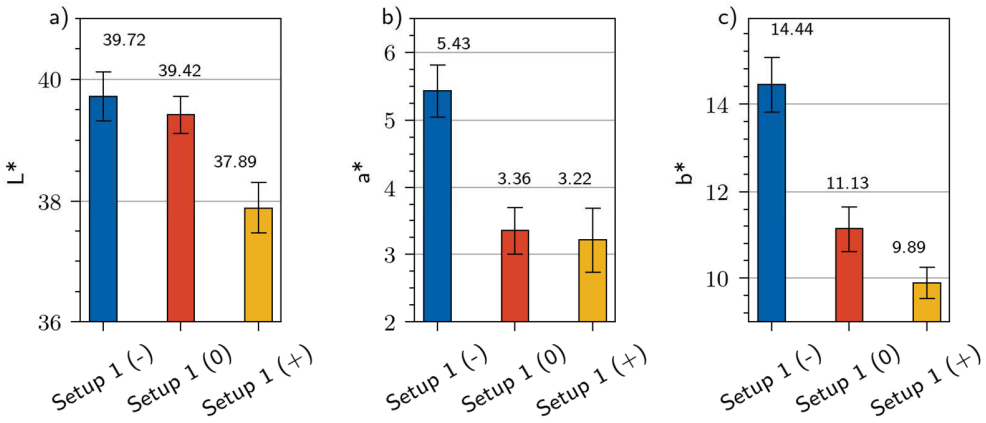

Figure 10: L*a*b* component for flax epoxy biobased composites made with setup 1

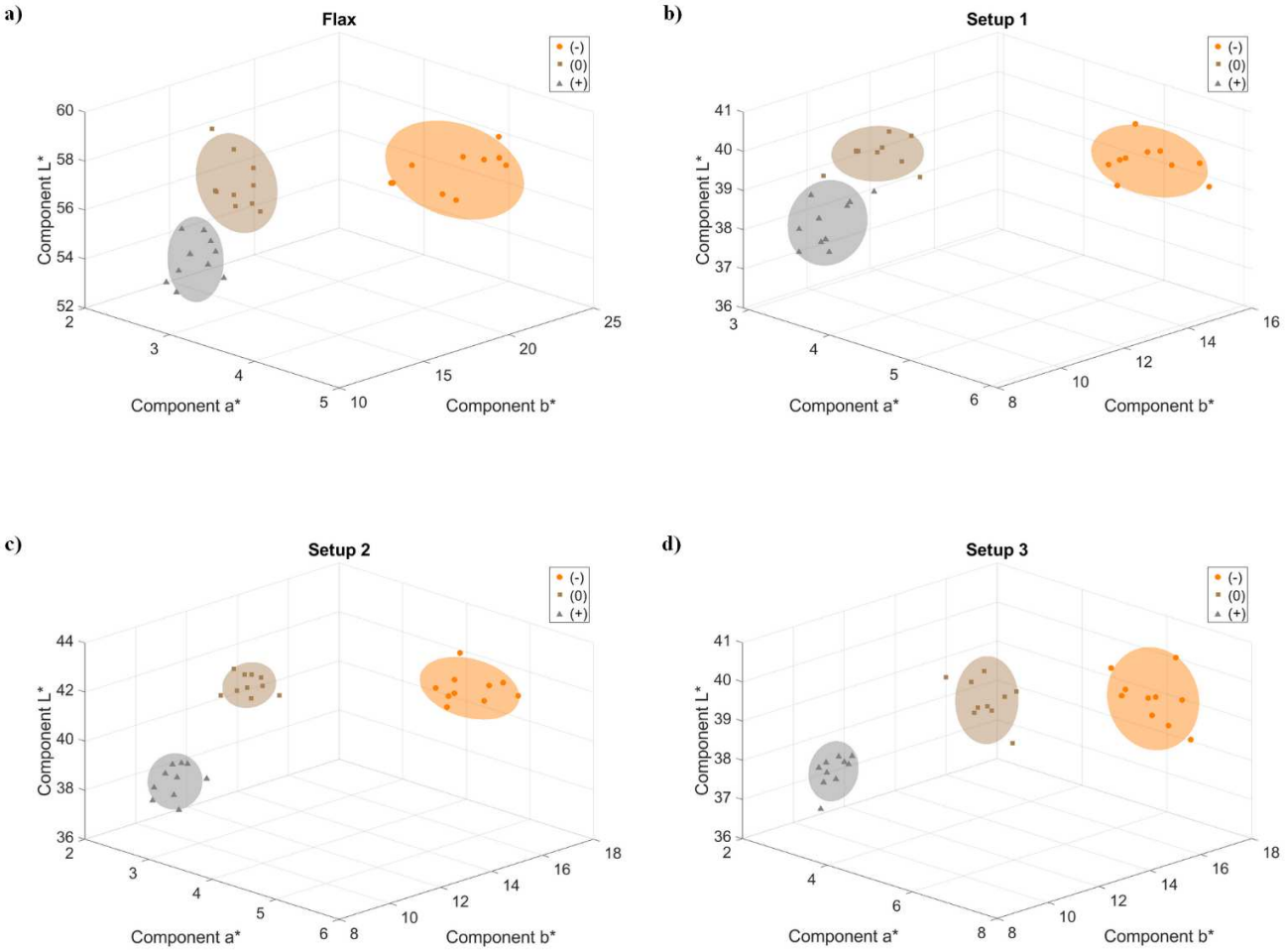

Figure 11: Spatial representation of L*a*b* components for a) flax, b) setup 1, c) setup 2, d) setup 3 (Made with Matlab software)

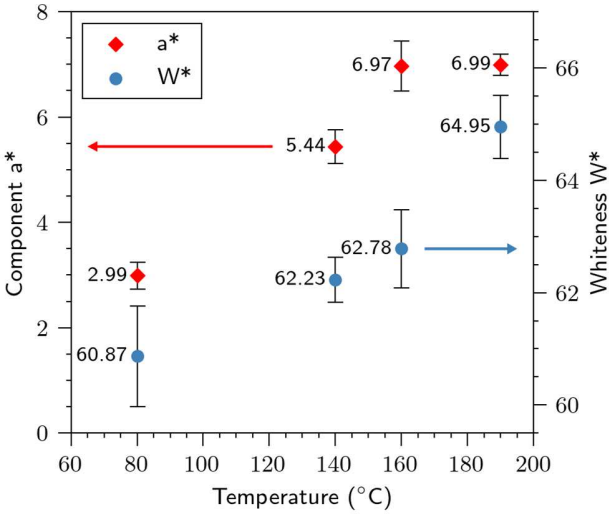

Figure 12: Effect of processing temperature on a* component and Whiteness Index

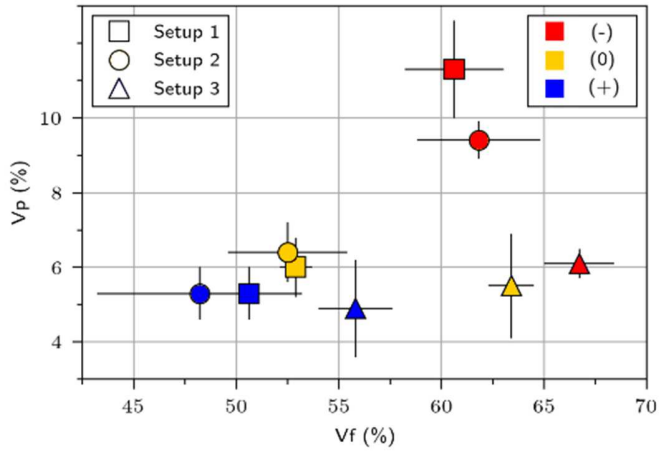

Figure 13: Biobased composite porosities versus experimental V_f

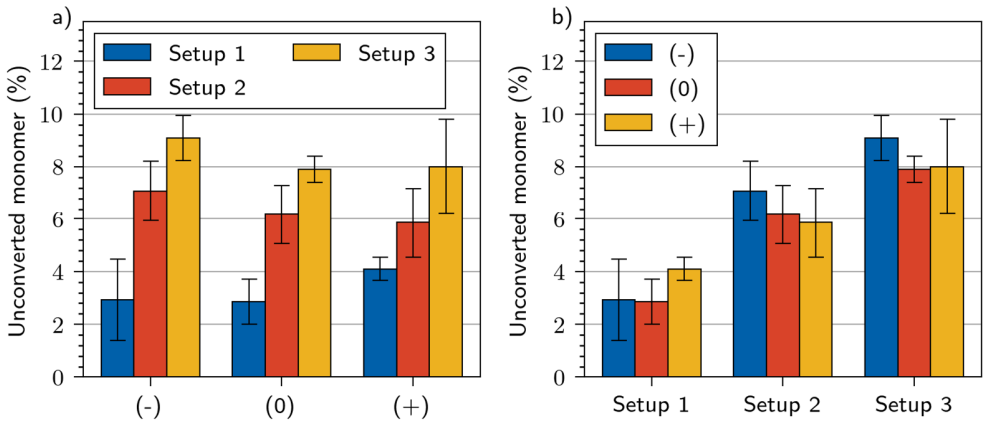

Figure 14: Curing efficiency of biobased composites a) Processing influence b) Retting influence.

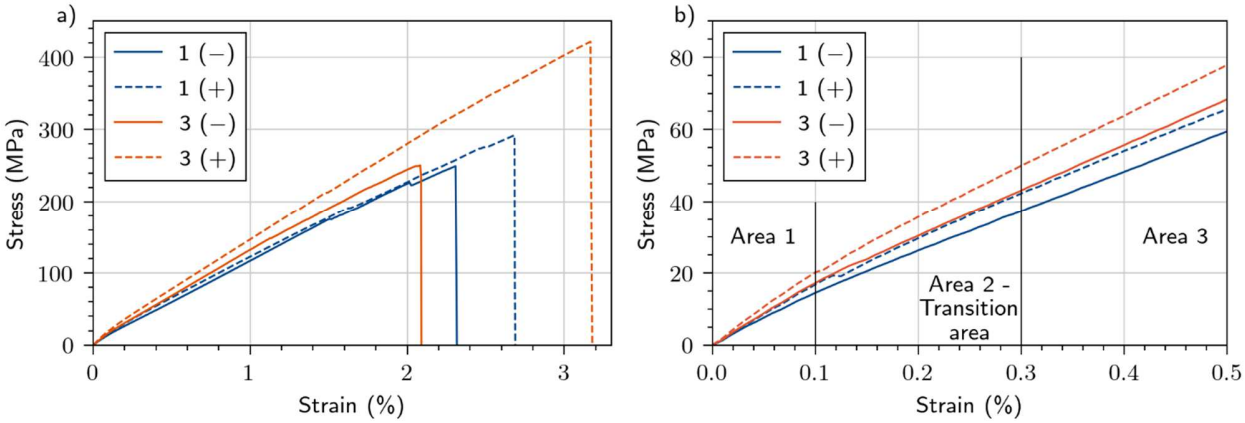

Figure 15: Stress-strain curves of biobased composites a) Global curve, b) Zoom in small deformations area.

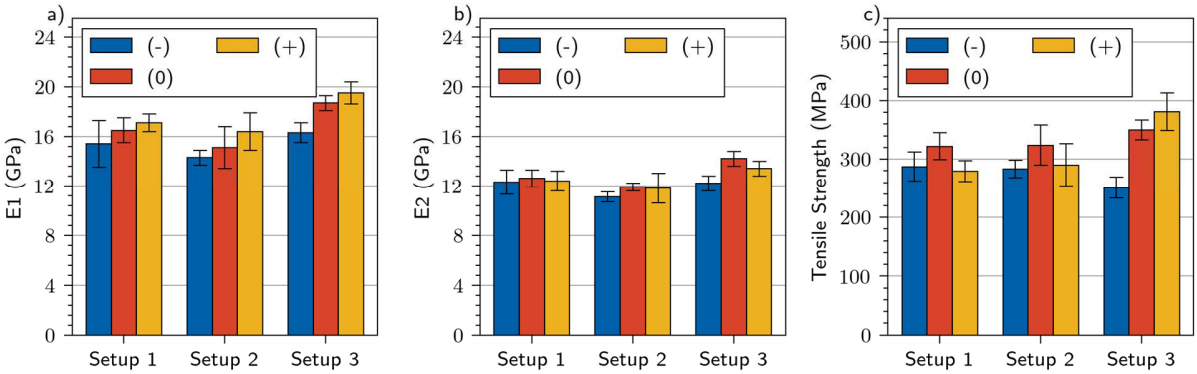

Figure 16: Influence of retting and setup on raw mechanical properties a) E1 modulus, b) E2 modulus, c) Maximal stress,

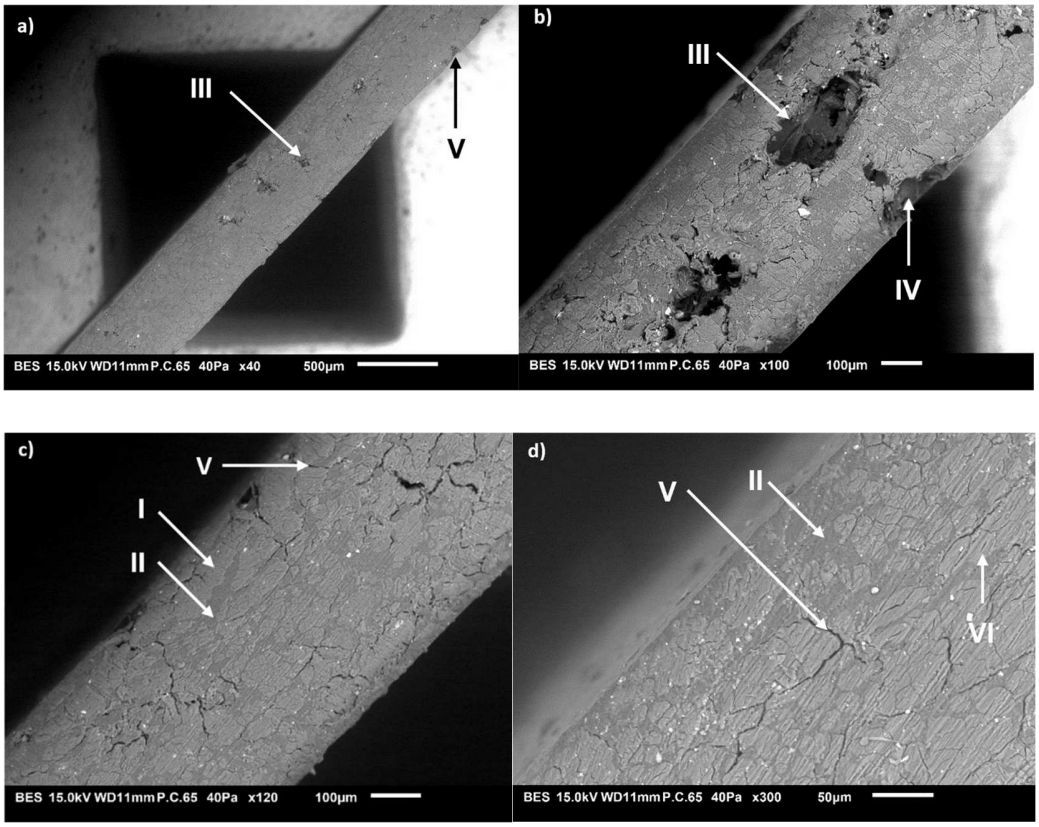

Figure 17: SEM pictures of the composite 2 (-) with magnification X40, X100, X120 and X300 - flax fibres (i), epoxy matrix (ii), structural porosity or dry area (iii), open porosity (iv), interfacial porosity (v), lumen (vi)

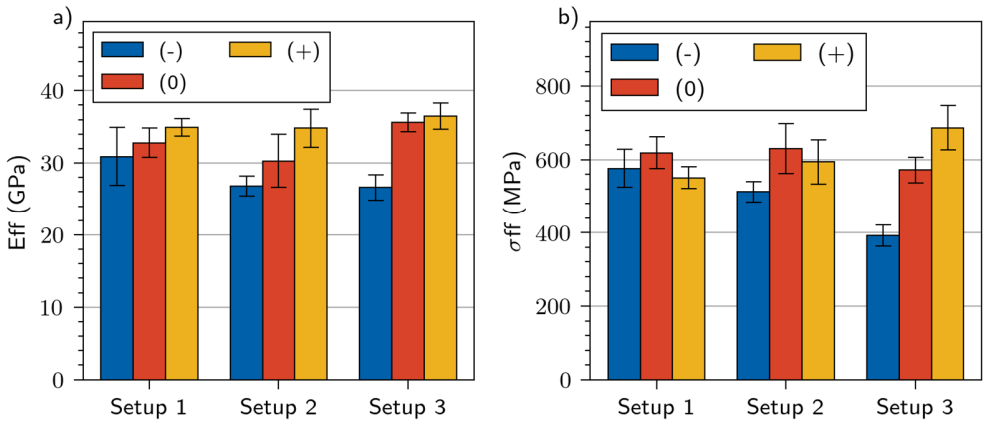

Figure 18: Influence of retting and setup on effective mechanical properties of reinforcement a) effective modulus- E_{ff}, b) effective strength-σ_{ff}

Table 1 : Data of cultivation and retting (detailer)

Retting	Seeding	Harvesting	Winding (W)	Total precipitation (mm)
Under retted (-)			W1 = 07/08/2017	17,2
Nominally retted (0)	10/04/2017	13/07/2021	W2 = 28/08/2017	66
Over retted (+)			W3 = 22/09/2017	130

Table 2 : Biobased composite manufactures

Setup	Retting	Times (min)	T max (°C)	P max (Bars)	Thickness (µm)	Area density ($g.m^{-2}$)
1	(-)	370	140	50	495 ± 21	685 ± 29
1	(0)	370	140	50	485 ± 22	654 ± 30
1	(+)	370	140	50	473 ± 13	634 ± 17
2	(-)	175	140	25	553 ± 15	766 ± 21
2	(0)	175	140	25	524 ± 18	706 ± 25
2	(+)	175	140	25	485 ± 19	647 ± 25
3	(-)	130	160	50	506 ± 24	704 ± 33
3	(0)	130	160	50	458 ± 13	631 ± 18
3	(+)	130	160	50	458 ± 10	620 ± 13

Table 3 : Mechanical properties of technical flax fibers

Modalities	Extrapolations to 0mm length			Extrapolations to 100mm length		
	(-)	(0)	(+)	(-)	(0)	(+)
Young's modulus (GPa)	68.9	77.1	88.2	66.8	58.6	41.3
Tensile Strength (MPa)	631	612	553	477	350	224
Failure strain (%)	1.07	1.03	0.85	0.86	0.76	0.69

Table 4: Weight and volumic composition of biobased composites

Composite	W_f	V_f	V_m	V_p	V_w
1 (-)	72.97 ± 2.22	60.57 ± 2.07	24.13 ± 2.07	11.28 ± 1.23	4.06 ± 0.31
1 (0)	61.47 ± 0.50	52.90 ± 0.45	37.19 ± 0.45	6.00 ± 0.80	3.90 ± 0.15
1 (+)	58.60 ± 2.57	50.56 ± 2.34	40.56 ± 2.34	5.30 ± 0.70	3.59 ± 0.14
2 (-)	79.99 ± 3.09	61.80 ± 2.89	24.15 ± 2.89	9.42 ± 0.48	4.63 ± 0.41
2 (0)	61.26 ± 2.94	52.47 ± 2.68	37.37 ± 2.68	6.45 ± 0.80	3.71 ± 0.72
2 (+)	56.24 ± 5.11	48.24 ± 4.62	42.32 ± 4.62	5.30 ± 0.71	4.13 ± 0.32
3 (-)	75.65 ± 1.57	66.75 ± 1.48	22.26 ± 1.48	6.11 ± 0.32	4.87 ± 0.71
3 (0)	71.75 ± 0.10	63.40 ± 0.09	27.34 ± 0.09	5.54 ± 1.39	3.72 ± 0.48
3 (+)	63.81 1.50	55.83 ± 1.38	35.17 ± 1.38	4.90 ± 1.25	4.11 ± 0.58

Table 5 : Raw and normalized data

Composite	Fiber raw data			Matrix	Fiber effective properties	
	E 1 (GPa)	E 2 (GPa)	σ (MPa)	Em (GPa)	Ef (GPa)	σf (MPa)
1 (-)	15.42 ± 1.91	12.31 ± 1.02	287.4 ± 25.3	3.5	30.91 ± 4.01	576.0 ± 52.4
1 (0)	16.45 ± 0.98	12.57 ± 0.74	322.2 ± 23.1	3.5	32.84 ± 2.02	619.1 ± 42.6
1 (+)	17.08 ± 0.96	12.37 ± 0.76	279.1 ± 17.9	3.5	34.87 ± 1.24	550.8 ± 29.0
2 (-)	14.29 ± 0.58	11.11 ± 0.42	283.1 ± 14.5	3.5	26.82 ± 1.37	511.6 ± 27.6
2 (0)	15.09 ± 1.69	11.89 ± 0.28	323.5 ± 33.9	3.5	30.34 ± 3.67	630.1 ± 68.1
2 (+)	16.38 ± 1.46	11.83 ± 1.23	290.2 ± 36.1	3.5	34.87 ± 2.58	594.1 ± 59.7
3 (-)	16.30 ± 0.83	12.18 ± 0.65	250.9 ± 16.2	3.5	26.61 ± 1.84	392.4 ± 29.1
3 (0)	18.68 ± 0.57	14.20 ± 0.57	350.0 ± 17.4	3.5	35.59 ± 1.31	572.0 ± 34.5
3 (+)	19.48 ± 0.91	13.42 ± 0.59	381.6 ± 32.1	3.5	36.52 ± 1.82	687.4 ± 59.5